Regeneration of Cochlear Hair Cells in Adult Mice by Chemical Mediated Reprogramming

Yi-Zhou Quan
Massachusetts Eye and Ear Infirmary
Wei Wei
Department of Otology and Laryngology, Harvard Medical School
Volkan Ergin
Department of Otology and Laryngology, Harvard Medical School
Arun Prabhu Rameshbabu
Department of Otology and Laryngology, Harvard Medical School https://orcid.org/0000-0001-8599-569X
Mingqian Huang
Department of Otology and Laryngology, Harvard Medical School
Chunjie Tian
Department of Otology and Laryngology, Harvard Medical School
SV Saladi
Mass Eye&Ear Infirmary
Artur Indzhykulian
Harvard Medical School https://orcid.org/0000-0002-2076-6818
Zheng-Yi Chen (Zheng-Yi_Chen@meei.harvard.edu)
Department of Otology and Laryngology, Harvard Medical School https://orcid.org/0000-0002-1452-4193

Article

Keywords:

Posted Date: June 3rd, 2022

DOI: https://doi.org/10.21203/rs.3.rs-1662674/v1

Title

Regeneration of Cochlear Hair Cells in Adult Mice by Chemical Mediated Reprogramming

Authors

Yi-Zhou Quan[1,2]†, Wei Wei[1,2,4]†, Volkan Ergin[1,2]†, Arun Prabhu Rameshbabu[1,2], Mingqian Huang[1,2], Chunjie Tian[1,2], SV Saladi [2,3], Artur A Indzhykulian[1,2], and Zheng-Yi Chen[1,2]*

Affiliations

[1]Department of Otolaryngology-Head and Neck Surgery, Graduate Program in Speech and Hearing Bioscience and Technology and Program in Neuroscience,
Harvard Medical School, Boston, MA 02115.
[2]Eaton-Peabody Laboratory, Massachusetts Eye and Ear Infirmary, 243 Charles St., Boston, MA 02114
[3]Broad Institute of MIT and Harvard, Cambridge, Massachusetts 02142, USA.
[4]Department of Otolaryngology-Head and Necks, Shengjing Hospital of China Medical University, Shenyang, 110004, China
†These authors contributed equally
*Corresponding author: Zheng-Yi_Chen@meei.harvard.edu

Abstract

Strategies to overcome irreversible cochlear hair cell (HC) damage and loss are of vital importance to develop treatment for hearing loss. In mature mammalian cochlea, *Myc* and *Notch1* co-activation reprograms supporting cells (SC) for HC regeneration. To understand the mechanisms underlying reprogramming, we performed single cell RNAseq and uncovered the pathways including Wnt and cAMP, whose blockade attenuate HC regeneration. We screened and identified a combination (the cocktail) of drug-like compounds of small molecules and siRNAs to activate the pathways of *Myc, Notch1, Wnt and cAMP*. We show that the cocktail effectively replaces *Myc* and *Notch1* transgenes to reprogram adult wildtype supporting cells for HC regeneration *in vitro*. Finally, we demonstrate the cocktail is capable of reprogramming adult cochlea for HC regeneration in wildtype mice with hair cell loss *in vivo*. Our study identified a strategy by a clinically-relevant approach to reprogram mature inner ear for HC regeneration, laying the foundation for hearing restoration by HC regeneration.

MAIN TEXT

Introduction

Hearing loss affects one in 500 newborns and half of the population over 70 years old, worldwide [1,2]. Despite being one of the most common forms of human sensory deficits, there is currently no pharmacological therapy for hearing loss. The mammalian inner ear detects the sound through the function of hair cells, the sensory cells that convert sound signals into electrical impulses [3]. Hair cell loss is considered the major cause of hearing loss [4,5]. However, the mammalian inner ear does not have the capacity to spontaneously repair or regenerate hair cells after hair cell damage or loss, leading to permanent hearing loss.

To use HC regeneration for hearing restoration, different strategies have been pursued. Various evidence suggests that HC regeneration in mammals is possible. Spontaneous HC regeneration occurs in lower vertebrates like birds and fish [2,6,7]. Embryonic and neonatal mouse cochlea also retains the capacity to regenerate HCs by enhancing expression of specific genes essential for HC development [8-10]. Activating Sonic Hedgehog signaling resulted in cell cycle re-entry and HC in the neonatal cochlear sensory epithelium [11,12]. The ERBB2 pathway was shown to promote supporting cell proliferation with increased MYO7A$^+$ cell generation in neonatal mice [13]. However, the capacity to generate HCs decreases rapidly 2 weeks after birth, even with the manipulation of multiple signal pathways [9]. Specifically none of the approaches were sufficient to regenerate HCs in the adult mouse cochlea.

To achieve HC regeneration in adult cochlea, we hypothesized a two-phase process could be sufficient: 1) To reprogram mature cochlear SCs to regain the properties of their young biological selves; 2) To activate a HC fate-determining factor (*Atoh1*) in the reprogrammed adult SCs for HC regeneration. We have shown that, by transient co-activation of *Myc* and *NICD* (*Notch1 intracellular domain),* the adult mouse cochlea can be successfully reprogrammed to a relatively younger stage and regain progenitor capacity, with regeneration of HCs following *Atoh1* overexpression *in vitro* and *in vivo* [14]. In the study, reprogramming and HC regeneration were achieved through the manipulation of the transgenes of *Myc* and *Notch1* in a transgenic mouse model. However, it remains a major challenge to develop a similar strategy for HC regeneration in the WT mature inner ear that is potentially clinically applicable.

To identify molecules to reprogram mature cochlear SCs, we performed single cell RNAseq and uncovered the pathways and their target genes underlying MYC/NICD mediated reprogramming. We screened small chemical compounds and small interfering RNAs (siRNA) to target downstream pathways and genes. Using a cocktail composed of small molecules and siRNAs, we demonstrate that *Myc* and *Notch1* genes can be effectively replaced to reprogram terminally differentiated mature cochlear epithelial cells, including SOX2$^+$ supporting cells (SCs), which regain progenitor properties and efficiently transdifferentiate into HCs in the adult inner ear *in vitro*. Significantly the strategy is shown to regenerate HCs in the wildtype adult mouse inner ear following HC loss *in vivo.* Our data suggest that regeneration of cochlear HCs can be achieved in adult mice using a drug-like approach offering a clinical potential.

Results

Replacement of MYC by siRNAs and NOTCH1 by VPA (valproic acid)

Mature cochlear epithelial cells lack the capacity to respond to the HC induction signals of *Atoh1* overexpression or *Rb* inhibition to regenerate HCs [9,15]. We have shown that regeneration of HC in the mature cochlea in a transgenic mouse model (rtTA/tet-Myc/tet-NICD) [14] (Supplementary Fig. 1) by reprogramming through transient activation of MYC/NICD followed by HC induction by Ad.*Atoh1* infection [14].

To advance our approach towards potential clinical application, it is necessary to reprogram supporting cells in the wildtype (WT) non-transgenic mature mammalian inner ear by a clinically relevant method that is sufficient to replace the functions of transgenes *Myc* and *Notch1*.

Valproic acid (VPA), a histone deacetylase inhibitor, is a well-known Notch activator in multiple organs [16,17] and is capable of expanding the sensory progenitors in neonatal cochleae [18]. We hypothesized that VPA may sufficiently activate *Notch1* in reprogramming the mature mouse cochlea. To test the hypothesis, we bred rtTA/tet-*MYC* mice with Atoh1-GFP reporter mice to create an rtTA/tet-*MYC*/Atoh1-GFP model. The cultured adult rtTA/tet-*MYC*/Atoh1-GFP cochleae were treated by Doxycycline (Dox) to activate *Myc* and VPA for four days followed by addition of ad.*Atoh1* in culture (Fig. 1a). 14 days after Ad.*Atoh1* infection, numerous HC-like cells ($MYO7A^+/GFP^+$) were generated (Fig. 1c1-c3; d-g). In contrast, in cultured adult rtTA/tet-*MYC*/Atoh1-GFP cochlea infected with ad.*Atoh1* alone, sporadic infected cells (GFP^+) became HCs (Fig. 1b-b3; d-g). To study the new HCs, we performed scanning electron microscopy (SEM) to identify kinocilia, a HC structure that only presents in the neonatal cochlear HCs [19]. Indeed, regenerated immature HCs with and without kinocilia were detected (Fig. 1h-k) in the VPA/Dox/adAtoh1 treated rtTA/tet-*MYC* cochleae, an indication of new HCs. Regenerated HCs were labeled with an additional HC marker ESPN (Fig. 1l-o). Some $ESPN^+$ HCs were also labeled with a SC marker SOX2 (Fig. 1l-o, arrows), supporting the regenerated HCs of SC origin. Importantly, a similar number of HCs were regenerated in the sensory epithelium and the limbus region between the VPA/Dox treated rtTA/tet-*Myc* and Dox treated rtTA/tet-*Myc*/tet-*NICD* adult cochleae (Fig. 1e vs. Supplementary Fig. 1c; Fig. 1g vs. Supplementary Fig. 1d), supporting that VPA effectively replaces NICD in reprogramming adult cochlea with *Myc* for HC regeneration.

Since there is no potent small molecule activators of *Myc,* we seek to activate *Myc* by the suppression of *Myc* suppressors using siRNA. We tested the siRNAs for the *Myc* suppressors *Fir* (siF) and *Mxi1* (siM) [20,21] in cultured adult cochlea. The siRNAs for *Fir* and *Mxi1* suppressed the respective gene and importantly, when combined, this resulted in *Myc* activation (Supplementary Fig. 2a). We then combined VPA and two species of siRNAs (siFsiM) to treat cultured WT adult cochlea to activate *Notch1* and *Myc* for reprogramming for four days followed by administration of Ad.*Atoh1-mCherry* for 14 days (Supplementary Fig. 2b). New $MYO7A^+$/Atoh1-$mCherry^+$ HCs were detected in the adult mouse cochlea (Supplementary Fig. 2c, d). However, compared to HC regeneration in the rtTA/tet-*Myc*/tet-NICD model (Supplementary Fig. 1c), the regeneration efficiency by VPA/siRNAs is greatly reduced. We conclude that VPA and the *Fir/Mxi1* siRNAs can partially replace *Notch1* and *Myc.* To improve HC regeneration efficiency, further manipulations will be necessary.

Single cell RNAseq reveals diverse cellular response to *Myc/NICD*-mediated reprogramming

Uncovering the downstream pathways mediated by MYC/NICD will aid our understanding of the reprogramming mechanisms and importantly provide us with the knowledge to identify an avenue for a clinically relevant strategy for HC regeneration. We used an adult cochlea explant culture

system we previously developed [14] and single-cell RNAseq to study the global gene expression profiles of the transgenic mouse model, rtTa/tet-*Myc/-tet-NICD,* in response to Dox-induced MYC/NICD co-activation. We have shown that a 4-day treatment by Dox in cultured adult rtTa/tet-*Myc/-tet-NICD* cochleae was sufficient to reprogram adult SCs for HC regeneration [14]. We thus treated cultured adult rtTa/tet-*Myc/-tet-NICD* cochleae with Dox for four days before the harvest to create cDNA libraries for NGS processing (Control, sterile water, n=4; and Dox-administered, n=8) (Fig. 2a and Methods). By CellRanger pipeline, we acquired single-cell transcriptomes in a total of 512 cells from Control samples and 1883 cells from Dox-treated samples (Supplementary Fig. 3a). Following filtering (Supplementary Fig. 3b) by the Seurat v.3.2 [22], the scRNA-seq data were clustered by the principal component which identified 9 distinct clusters. Based on the previous single-cell RNAseq studies in the cochlea [23-27], the clusters were assigned: interdental cells (IdC), Claudius cells/outer sulcus cells (CCOS), Reissner's membrane cells (RMC), Deiter's cells (DC), Kolliker's organ cells (KO), Hensen's cells (HeC), unclassified-supporting cells (uSC), macrophage-like cells (MLC) and hair cells (HC) (Fig. 2c). When comparing Dox treated and control samples, *Myc* and *Notch1* were upregulated in Dox-treated cells (Fig. 2d, e). The cell identities of each cluster were associated with known cell type marker gene expression (Supplementary Fig. 4a, Table S1), including Galm, Nfix, Epcam for IdC; Cp, Col3a1, Fstl1 for CCOS; Vmo1, Meis2, Fut9 for RMC; Bace2, Caecam16, Car14 for DC; Epyc, Slc39a8, Lum for KO; Plp1, Pmp22, Sostdc1 for HeC; Cx3cr1, Emilin2, Fcgr1 for MLC; and Pvalb, Atp8a2, Nefl for HC (Supplementary Fig. 4b, c). For the cluster uSC, genes such as Gdf15, Ciart, Hspa1a could not be assigned to an existing known cluster within the cochlea, indicating the cluster may contain the cells whose expression profiles were drastically altered by culturing conditions and/or Dox treatment. We did not detect certain cochlear cell types such as pillar cells, stria vascularis cells, or phalangeal cells. In summary, we profiled the transcriptomes of most cell types in the cultured adult cochlea with and without *Myc/Nocth1* activation.

Identification of the *Myc/Notch1* downstream pathways in reprogramming

We performed differential gene expression analysis and pathway enrichment analysis to characterize the molecular signature during reprogramming (Supplementary Fig. 5). First, we observed almost no overlap of differentially expressed genes (DEGs) between the two groups (Supplementary Fig. 5a, Table S2), suggesting that co-activation of *Notch1* and *Myc* profoundly affects overall gene expression of the cultured cochlea. By Gene Set Enrichment Analysis [28,29], we identified genes enriched under *Myc/Notch1* co-activation in the pathways including MYC targets and NOTCH signaling, E2F targets, G2M checkpoint, oxidative phosphorylation, and mTORC1 (Supplementary Fig. 5b). We visualized the genes from the top 5 Hallmark sets and found the interdental cell (IdCs) cluster to have the most distinct expression profiles that were high in the Dox treated compared to the control groups (Supplementary Fig. 5c), suggesting that the interdental cells were more sensitive to MYC/NICD co-activation than other cochlear cell types. The pathways highly activated in the interdental cells such as E2F targets and G2M are involved in proliferation. We tested the hypothesis that the interdental cells were more sensitive to MYC/NICD co-activation to proliferate by studying EdU incorporation in the cultured adult rtTA/tet-MYC/tet-NICD cochlea treated with Dox. In the limbus region (the IdC cluster), a greater number of EdU^+ cells were observed compared to other cell types such as the sensory epithelium (SE) (Supplementary Fig. 5d, e).

In addition to a greater proliferation potential, the IdCs have the highest regeneration potential among the cochlear cell types *in vitro* (Supplementary Fig. 1b3) and *in vivo* [14], suggesting that the IdCs responded to reprogramming more efficiently, and as the consequence transdifferentiated to HCs more readily in the presence of *Atoh1*. To study the IdC clusters based on RNAseq in detail, we selected the IdC clusters for subclustering (Fig. 3a). To infer the timing of gene activity in IdC

reprogramming following Dox induction, we performed pseudotime trajectory analysis using Monocle3 [30,31] to reveal gene expression kinetics over time in single-cell resolution. Based on the trajectory, the cells were then ordered in pseudotime by defining a starting node where the most of the IdC_Control cells without reprogramming resided (Fig. 3b), and an ending node represented by the reprogrammed IdC_Dox cells (Fig. 3b). The pseudotime trajectory of the reprogramming process curated 4 distinct regulatory modules with the genes (Table S3) that co-expressed across individual cells, and each module containing a set of co-regulated genes corresponds to a unique state during the transition from IdC_Control to IdC_Dox state (Fig. 3c).

We performed pathway analysis by DAVID on the list of co-regulated genes in each of 4 modules revealed by Monocle3 [30,31]. DAVID identified that in Module 1 representing the baseline state of un-reprogrammed IdCs control, chromatin silencing and epigenetic regulations were more prominently expressed (Supplementary Fig. 6a). In Module 2, the genes representing an early transition state were mostly cytoskeletal and post-translational modification regulatory genes such as kinases, nucleosome and ubiquitin-conjugation enzymes (Supplementary Fig. 6b). In Module 3 of a late transition state, the genes classified as extracellular matrix or cell-cell adhesion-related genes were enriched (Supplementary Fig. 6c). Lastly, in Module 4 representing the Dox-induced reprogrammed state, co-regulated genes were enriched for transcriptional regulation, morphogenesis, development, and mechanosensing (Fig. 3d), which indicated the prominent gene classes contributing to reprogramming and/or differentiation capacity of the reprogrammed IdC cells by MYC/NOTCH co-activation.

In Module 4, GO analysis identified Wnt and cAMP-induced signaling as highly represented (Fig. 3d), suggesting these pathways may play significant roles in the acquisition and establishment of the reprogrammed-state of the IdCs by Dox induction. To better evaluate the relationship of Wnt and cAMP pathway genes in the IdC clusters between Control and Dox samples, we plotted gene expression profiles of selected Wnt and cAMP pathways genes from Module 4 as a function of pseudotime (Fig. 3e). Ten representative genes for the Wnt pathway or cAMP-response pathway showed a gradual increase in their expression levels during transition from Control to the reprogrammed state by Dox induction, supporting that these pathways are part of reprogramming process. Using the STRING tool [32], we constructed a protein-to-protein interactive network composed of Wnt- and cAMP-related genes connected by *Ccnd1* (Fig. 3f). Overall, we found that IdCs are highly sensitive to MYC/NICD induced reprogramming, which may underlie their heightened potential to transdifferentiate to HC.

Wnt and cAMP are downstream of MYC/NICD-mediated reprogramming and are necessary for HC regeneration.

Identification of Wnt and cAMP upon MYC/NICD activation suggests the important roles for each pathway in HC regeneration in mature cochlea. To confirm the results from the single-cell RNA-seq study, we measured the expression of selected Wnt and cAMP pathway genes by qRT-PCR in cultured adult rtTA/tet-*Myc*/tet-NICD cochlea after Dox treatment and detected upregulation of Wnt and cAMP pathways genes in the Dox treatment group (Supplementary Fig. 7). To determine if Wnt and/or cAMP is required for MYC/NICD-mediated reprogramming for HC regeneration, we activated MYC/NICD in cultured adult rtTA/tet-*Myc*/tet-NICD cochlea, in the presence of small molecule Wnt inhibitor IWP2, cAMP inhibitor BI (bithionol), or both IWP2+BI [33,34], with the cochleae subsequently infected by Ad.*Atoh1-mCherry*. In control cochlea without Wnt or cAMP inhibitors, MYC/NICD reprogrammed adult cochlear cells in the sensory epithelium and the limbus region and responded to *Atoh1* to transdifferentiate to HC efficiently (Supplementary Fig. 7c-e). In the cochlear groups treated with the Dox+IWP2, Dox+BI or Dox +IWP2+BI, HC regeneration was severely attenuated despite the presence of abundant Ad.*Atoh1-mCherry* infected cells in the

sensory epithelium and the limbus region (Supplementary Fig. 7c-e). The Bi/Iwp2 combination had stronger inhibitory effect than BI or Iwp2 alone in the sensory epithelial region (Supplementary Fig. 7e). Taken together, we demonstrated that in adult mouse cochlea, Wnt and cAMP pathways were activated by MYC/NICD activation, and both are necessary for reprogramming of adult cochlear cells and their transdifferentiation to HC in the sensory and non-sensory epithelium.

Regeneration of HCs by the cocktail-driven reprogramming in wildtype adult mouse cochlea *in vitro*.

The necessity of Wnt and cAMP in MYC/NICD mediated HC regeneration suggests their activation could facilitate HC regeneration. To maximize the efficiency in HC regeneration, we combined VPA, siFIR, and siMxi1 (VsiFsiM) with a Wnt agonist LiCl(L) and a cAMP agonist Forsklin (FSK, F) to constitute a VLFsiFsiM "cocktail". We tested reprogramming by applying the cocktail to cultured adult WT cochleae and studied activation of inner ear progenitor genes. qPCR showed upregulation of progenitor genes including *Six1, Eya1* and *Gata3*, but not embryonic stem cell genes like *Nanog* and *Fut4* (Supplementary Fig. 8a, b), mimicking the reprogramming effect of MYC/NICD in the transgenic mice [14].

To determine if the VLFsiFsiM cocktail is sufficient to reprogram adult WT cochlea for HC regeneration, we added the cocktail to cultured adult Atoh1-GFP mouse cochleae, in which the Atoh1 enhancer drives expression of a nuclear GFP reporter, allowing the tracking of the cells with *Atoh1* expression (Fig. 4a). Four days after the treatment by the cocktail, the adult cochleae were infected by an adenoviral vector carrying the *Atoh1* gene (Ad.*Atoh1*), and further cultured for 14 days. Ad.*Atoh1* infected a similar number of SC in the cocktail-treated and untreated control samples shown by GFP signal (Fig. 4a, b1, c1, d, f). In the cocktail-treated samples, we found numerous HCs (Atoh1-GFP$^+$/MYO7A$^+$) regenerated in the adult cochlear sensory epithelium (Fig. 4c; d-g). In contrast, in control adult Atoh1-GFP cochlea without cocktail treatment, Ad.*Atoh1* infection did not result in Atoh1-GFP$^+$/MYO7A$^+$ HCs (Fig. 4b; d-g). We performed lineage tracing study to determine the origin of new HCs. Using the Sox2CreER-tdTomato model in which tamoxifen exposure activates tdT permanently in the SOX2$^+$ SC, we found that after cocktail+Ad.*Atoh1* treatment, new HCs were co-labeled with tdT (arrowheads, Fig. 4h-j), demonstrating SC origin of regenerated HCs.

To study if the new HCs possess functional transduction channels, we performed FM1-43 uptake by regenerated HCs 14 days after Ad.*Atoh1* infection. FM1-43 is a fluorescent dye that passes through functional transduction channels and is trapped by its charge with HCs. We observed FM1-43$^+$/Atoh1-GFP$^+$/MYO7A$^+$ triple positive HCs in the cocktail treated group, indicating the uptake of the dye by new HCs (Fig. 4k). New HCs are positive for developing HC markers including POU4F3 and PCP4 (Supplementary Fig. 9a-c). Interestingly, we found some Atoh1-GFP$^+$/MYO7A$^+$ and POU4F3$^+$/PCP4$^+$ HCs in clusters with a sphere-like structures in the cocktail treated group (Fig. 4l; Supplementary Fig. 9c), reminiscent of the spheres derived from inner ear stem cells, suggesting our reprogramming process may expand stem cells/progenitors from which subsequently transdifferentiated to HCs. By scanning electron microscopy (SEM), we detected regenerated immature HCs with or without kinocilia (Supplementary Fig. 9d1-d3). Taken together, we demonstrated that the novel "VLFsiFsiM cocktail" is sufficient to reprogram the adult mouse cochlea in lieu of MYC/NICD transgenes and regenerate HCs in combination with *Atoh1*.

Hair cell regeneration by the VLFsiFsiM cocktail in a mouse model with hair cell loss *in vivo*

The cocktail approach to reprogram WT adult cochlea for HC regeneration *in vitro* supports its application for HC regeneration *in vivo.* To assess if the cocktail could be delivered by middle ear for reprogramming, we first tested by injecting the cocktail VLFsiFsiM into the middle ear space

in adult WT mice and collected the cochlea 4 days later to study the effect. qPCR showed the upregulation of *Myc, Notch1,* and inner ear progenitor markers by the cocktail (Supplementary Fig. 8c, d). To determine if the cocktail is sufficient for reprogramming and HC regeneration *in vivo,* we used a mouse model with severe HC loss induced by the ototoxic drug Kanamycin. We observed that, 7 days after intraperitoneal (i.p.) injection of Kanamycin and Furosemide, over 95% of OHCs were killed from apex-mid to middle turns, whereas the SCs ($SOX2^+$) were preserved in the same region, making it a good model to study HC regeneration in the OHC region *in vivo* (Supplementary Fig. 10a-c). Using this HC damage model, we reprogrammed the damaged cochlea by injecting the VLFsiFsiM cocktail into the middle ear for four days, followed by injecting Ad.*Atoh1-mCherry* into the middle turn of the cochlea via cochleostomy. 21 days after Ad.*Atoh1-mCherry* injection, in control cochlea treated with vehicle (0.5% DMSO), occasional $ESPN^+$ HCs were detected in the apex-mid that coincided with mCherry signals (Fig. 5b), an indication of regenerated HCs. No HC was regenerated in the apex to mid turn despite of abundant infected SCs. In contrast, in the cochlea with cocktail treatment, numerous $ESPN^+$/$mCherry^+$ HCs were seen from apex to the mid turn (Fig. 5c; Supplementary Fig. 11c; S. Movie). Virtually all regenerated HCs were in the OHC region as the result of Ad.*Atoh1-mCherry* infection that targeted SCs in the same region (Fig. 5c; Supplementary Fig. 11c). As the result of HC regeneration, there was a significant increase in the HC number in the OHC region in the cocktail treated cochlea (Fig. 5d). There was no change in the number of IHC due to the lack of Ad.*Atoh1-mCherry* infection in the region (Fig. 5e). Notably, many regenerated HCs were positive for SOX2 ($SOX2^+$/$ESPN^+$, Supplementary Fig. 11d), indicating their SC origin. Consistent with SC-to-HC transition, the total number of non-transdifferentiated SCs, i.e. $SOX2^+$/$ESPN^-$ SCs, was significantly reduced in the reprogramed cochlea (Supplementary Fig. 11e). Again, there is no change in the number of SCs in the IHC region (Supplementary Fig. 11f). Taken together, we demonstrated that the middle ear delivery of "VLFsiFsiM cocktail" is sufficient to reprogram the adult mouse cochlea and regenerate HCs in combination with *Atoh1* in a severe HC loss mouse model *in vivo*.

Discussion

In this study, we used single-cell RNAseq to uncover the pathways underlying the MYC/NOTCH-mediated reprogramming of adult mouse cochlea. We further used the information to identify a combinatory approach by drug-like molecules to achieve reprogramming and HC regeneration in mature inner ear *in vitro* and *in vivo* (Fig. 6 for summary).

HC regeneration in mature mammalian inner ear is a necessary step in order to develop a strategy to use HC regeneration to treat hearing loss. While most HC regeneration studies have focused on neonatal mice, recent studies by different groups including us have shown the feasibility of adult HC regeneration [8,10,13,14,35-38]. We have developed a two-step approach to achieve adult HC regeneration: 1). Transient co-activation of cell cycle activator *Myc* and inner ear progenitor gene *Notch1* to reprogram adult cochlear supporting cells; 2). Overexpression of a transcription factor *Atoh1* in the reprogrammed SCs which then transdifferentiate into HCs *in vivo* and *in vitro* [14].

For our ultimate goal to develop MYC/NICD/Atoh1 based HC regeneration with clinic application, it is required that *Myc/Notch* can be co-activated by drug-like molecules for reprogramming in WT non-transgenic adult inner ear for efficient HC regeneration. To recapitulate the effect of MYC/NICD, we envisioned a replacement of MYC and NICD by drug-like small molecules and siRNAs. VPA is an established histone deacetylase inhibitor and is a known Notch signal agonist [16,17]. Indeed, in the rtTA/tet-*Myc* mouse model, *Notch1* can be effectively activated with VPA, which with Dox-induced MYC activation, results in HC regeneration after Ad.*Atoh1* infection (Fig. 1b, c).

Given that there is no known small molecule that can activate *Myc* potently, we first evaluated the possibility of using siRNAs to suppress *Myc* suppressors as a way to activate MYC. The siRNAs for *Fir* and *Mxi1*, two known MYC suppressors, exert the effect of MYC activation and HC regeneration (Supplementary Fig. 2). However, the regeneration efficiency is relatively low compared to what was achieved by MYC activation in the transgenic mouse model.

To compensate the inefficient MYC activation by siRNAs, and to gain the insight into the mechanisms underlying reprogramming in adult cochlea, we sought to identify MYC/NICD downstream signaling pathways by single-cell RNAseq using the rtTA/tet-*Myc*/tet-NICD model in which Dox activates MYC/NICD robustly. We hypothesized the analysis will provide a comprehensive view of the reprogramming pathways, which in addition could offer us the opportunity to manipulate some of them with drug-like molecules, to overcome the deficiency in MYC activation by siRNAs for efficient reprogramming and HC regeneration.

The RNAseq analysis identified 9 transcriptionally distinct clusters of the major sensory epithelial cell types, most of which are characterized by the expression of marker genes [23-26]. The analysis failed to identify few cell types such as the pillar cells and phalangeal cells. This may be in part due to the effect of MYC/NICD that drastically altered the cell type identity. We used cultured adult cochleae, which may have some effect on cell type identity compared to acutely dissected cochleae. Another possibility is that after culture and dissociation some cell types were lost disproportionately. Overall, the identification of most of the known cell types compared to freshly dissected cochlea from other studies [23,25] and the presence of known marker gene expressions confirm the quality and comprehensiveness of our data.

The RNAseq data showed, following Dox-induced MYC/NICD activation, that the global transcriptional profiles of adult cochlear explants differed substantially from their control counterparts. The hallmark of MYC/NOTCH induced reprogramming is the heightened activities shown by genes in cell cycle and cell growth, which were enriched for genes involved in positive regulation of MYC target genes, E2F target genes, G2M cell cycle checkpoint genes, mitotic spindle genes, oxidative phosphorylation genes, MTORC1 and NOTCH signaling genes. A recent single cell RNAseq study on zebrafish spontaneous HC regeneration after HC damage identified numerous pathways that are activated during different phases of reprogramming [39]. Among the top identified pathways in zebrafish, many are shared with the reprogrammed adult mouse cochlea including the pathways in mitotic activities, oxidative phosphorylation, Notch and Wnt, supporting that those pathways are intrinsic to reprogramming and HC regeneration from zebrafish and mammals. However, some pathways we identified are unique to mouse, including cAMP, indicating the requirement of the pathways specifically for mammalian HC regeneration.

To gain insight into the transcriptional changes within cell types and to assess the origin of mitotically active cells in MYC/NICD-induced samples, we analyzed differential expression profiles of the highly represented MSigDB Hallmark genes across cell clusters. This analysis showed that distinct expression profiles for the Hallmark gene sets were more significantly enriched in the interdental cell (IdC) populations, suggesting that MYC/NICD co-activation has a greater influence on the IdCs than on other cell types.

In our studies (Supplementary Fig. 1)[14], we noticed high efficiency IdC to HC transdifferentiation in the limbus region, suggesting that the IdC may under deeper reprogramming induced by MYC/NICD, which renders them more responsive to HC induction signals. This observation is consistent with the highly represented Hallmark gene sets in the IdC cluster by RNAseq. To

characterize transcriptional events that are fundamental in IdC reprogramming, we utilized a pseudo-time trajectory that allows for construction of the co-regulated transcriptional networks during transition between cell types and/or developmental stages. We identified four transcriptionally distinct subgroups of adult IdCs, depicted as transition stages from naive IdCs (Module #1) to the reprogrammed state (Module #4) (Fig. 3b, c). The GO analysis of Module #4, the reprogrammed state, identified Wnt and Response to cAMP as two enriched signaling pathways, suggesting their involvement in MYC/NICD-mediated reprogramming. By qPCR we confirmed the expression kinetics for the critical Wnt and cAMP-related genes across pseudo-time differentiation states of IdCs (Supplementary Fig. 7b). By the blockade of Wnt and cAMP pathways via small molecule inhibitors, cochlear HC regeneration or IdC proliferation potential is greatly attenuated despite MYC/NICD activation, demonstrating that Wnt and cAMP are downstream of MYC/NICD and are necessary for HC regeneration in the cultured adult cochlea (Supplementary Figs. 5; 7). While the IdC cluster was used to identify the reprogramming pathways, blockade of the pathways led to a significant reduction in regenerated HCs in the cochlea sensory epithelium, which strongly supports the relevance of the pathways in reprogramming the sensory epithelium and in HC regeneration.

The discovery of Wnt and Response to cAMP pathways as downstream of MYC/NICD made it possible to activate both pathways by small molecules: LiCl to activate Wnt and Forskolin (FSK) to activate cAMP. Wnt is a well-studied pathway in the inner ear development and hair cell regeneration although its role in adult HC regeneration is not yet clear [40,41]. Lithium chloride (LiCl) is a Wnt signaling agonist widely used in reprogramming terminally differentiated somatic cells into pluripotent stem cells (iPSCs) [42,43]. Application of LiCl causes the expansion of the prosensory domain with increased number of HCs in the embryonic mouse cochlea [41]. Interestingly, *Myc,* together of *Notch* in activating Wnt for reprogramming in adult cochlea, is also a known downstream target of the Wnt signal pathway [44,45]. Clearly there is a complexed cross-talk between the pathways exerting the effect in both directions. cAMP was reported in the induction of expansion the auditory epithelium in both birds and mammals in HC regeneration [46-48]. Forskolin (FSK) is the adenylate cyclase activator of cyclic AMP (cAMP) and has been utilized in replacing Yamanaka factors (YFs) in the protocol for chemical-induced pluripotent stem cells (CiPSCs) [49-51].

In our cocktail, we combined five components of VPA, LiCl, FSK and siRNA for Fir and Mxi1 to completely replace *Myc* and *Notch* transgenes for reprogramming in cultured adult WT cochlea. We detected HC regeneration after Ad.*Atoh1* infection, with the efficiency that is similar to HC regeneration achieved in the rtTA/tet-*Myc*/tet-NICD mice, which is more efficient than that achieved by VPA/siF/siM, demonstrating added reprogramming effect of LiCl and FSK. The study further illustrates that the reprogramming pathways identified in the IdC cluster are relevant to HC regeneration in the cochlear sensory epithelium. A combination of 13 chemicals has been shown to replace all 4 Yamanaka factors to reprogram somatic cells into pluripotent stem cells [49], which is likely involved deeper reprogramming. Our use of the cocktail with 5 components likely results in partial reprogramming, to allow fully differentiated SCs to regain a relatively young-age status, and to respond to *Atoh1* and transdifferentiate into hair cells.

Excitingly, in the severe HC loss mouse model, new HCs are regenerated from the "VLFsiFsiM" cocktail-treated reprogrammed SCs, compared to little HC regeneration in the vehicle-treated non-reprogrammed SCs. The data strongly support that a chemical-mediated reprogramming and HC regeneration can be achieved in the mature mammalian cochlea. For hearing restoration, it is required that the regenerated HCs be confined to the sensory epithelial region such that their stereocilia contact the tectorial membrane and mediate the mechanoelectrical transduction function. Our *in vivo* HC regeneration model under the condition of adenovirus infection directed the new

HCs to in the right place, i.e. new HCs were regenerated within the $SOX2^+$ sensory epithelium. Our next goal is to study how *in vivo* HC regeneration could lead to hearing recovery. This will likely require a different surgical procedure as cochleostomy used in the study is known to cause inner ear in particular HC damage. Further, the expression of *Aoth1* needs to be regulated as continuous *Atoh1* expression prevents HC maturation and induces HC death [9].

Our study is the first to show HC regeneration from cochlea long after HC loss in adult wild-type mice *in vivo*. Given the drug-like properties of our cocktail in reprogramming, this work strongly supports that the approach could be a viable therapeutic method to regenerate HCs, with an important implication for the development towards future clinical application.

Methods

Mouse models

Rosa-rtTA (rtTA), Sox2Cre transgenic mice and Ai14 tdTomato reporter mice were from Jackson Laboratory (Stock# 006965; 017593; 007914); tet-on-Myc mice were from Dr. M. Bishop of the University of California, San Francisco; tet-on-NICD mice were from Dr. D. Melton of Harvard University. For the transgenic rtTA/tet-on-Myc/tet-on-NICD mice, the background was mixed C57/129SvJ/CD1, with roughly equal numbers of sexes; Atoh1-nGFP mice were from Dr. Jane Johnson (University of Texas Southwestern Medical Center, Dallas, TX); the wild type mice were C57BL/6 from Jackson Laboratory. All experiments were performed in compliance with ethical regulations and approved by the Animal Care Committees of Massachusetts Eye and Ear and Harvard Medical School.

Adult cochlear culture and viral infection *in vitro*

Different from the neonatal cochlear culture method, in which the cochleae were disassociated from the bone, adult mouse whole cochleae (4-6 weeks old) were dissected with the bone attached. The bulla was first removed from the skull and dipped in 75% ethanol for 3 mins before being placed in HBSS. The vestibular region was also removed. Under a dissecting microscope, the middle ear, vessels and the debris were removed from the bulla. The bone covering the apical turn was removed, and round window and oval window membranes were opened to allow media exchange with the cochlear fluids. The ligament portion and Reissner's membrane at each end of the cochlea were also removed to facilitate the access of medium to the sensory epithelial region. The cochleae were maintained in DMEM/F12 (Invitrogen) supplemented with N2 and B27 (both from Invitrogen) for 14-18 days. Ad.*Atoh1*/Ad.*Atoh1-mCherry*/Ad.*Atoh1-GFP* adenoviruses were purchased from the SignaGen Laboratories, Rockville, MD, with titers of 6×10^{12} pfu/ml.

Single-cell preparation

Sensory epithelium from cochlea explants were dissected, and then dissociated immediately incubating with 0.25% trypsin-EDTA for 15 min at 37°C. Tissues were gently singularized by P1000 pipette in complete medium (DMEM/F12 medium containing 10% FBS). Cells were strained twice through 40 μm mesh into 5 ml medium, spun down for 5 min at 300 *g* to pellet and resuspend in 50 ml of complete medium. Roughly 1600 cells were loaded onto a 10X Chip-G for a target recovery of 1000 cells. Single cells from explant cochlear cultures of control (n=4) and Dox-treated (n=8) groups were captured separately to prepare two libraries.

Single-cell RNA library preparation and sequencing

Single cell suspensions were immediately transferred to individual channels of chip (Chromium Next GEM Chip G) to generate gel beads in emulsion together with reverse transcription master mix on the droplet-based high-throughput Chromium Controller (10X Genomics) allowing cell lysis, individual cell barcoding, and reverse transcription by Chromium Next GEM Single Cell 3' Kit v3.1 (10X Genomics, PN-1000128). Briefly, single cell library preparation was carried out by emulsion breakage, PCR amplification, cDNA fragmentation, oligo adapter, and Illumina sample index addition following the manufacturer's protocol. The single-cell derived cDNA libraries were then assessed with bioanalyzer (High Sensitivity DNA Kit, Agilent 2100 Bioanalyzer) for quality control. Following library preparation, next-generation sequencing was performed with paired-end sequencing of 150 bp each end using Illumina HiSeqXTen (Novogene Inc.).

Computational analysis of single-cell data

Transcriptome sequencing analysis and read mapping were performed using CellRanger pipeline (version 5.0.0; 10X Genomics) according to the manufacturer's guidelines. Raw sequencing reads

processed by CellRanger were demultiplexed and mapped to the mouse reference genome (mm10, GRCm38) using STAR. CellRanger-generated count matrices were loaded into Seurat v3.2.2 [22] for downstream analysis. Outlier cells were first identified based on three metrics (library size, number of expressed genes and mitochondrial proportion). Cells with less than 200 unique molecular identifiers or high mitochondrial content were filtered out. Datasets from each sample were integrated into a single matrix for comparative analysis with the integration workflow from Seurat using {Merge} function. After this, we performed global-normalization using the {SCTransform} function embedded in Seurat R package for normalization and scaling of UMI and mitochondrial content. For the unsupervised clustering, we chose 0.5 as the resolution parameter. Briefly, we performed the downstream analysis steps including {SelectIntegrationFeatures}, {PrepSCTIntegration}, {FindIntegrationAnchors}, {IntegrateData}, {RunPCA}, {RunUMAP}, {FindNeighbors} and {FindClusters} functions on the integrated dataset. Identification of differentially expressed cell type-specific markers was carried out in Seurat utilizing the {FindAllMarkers} function. Using this function, cells from each cluster were compared against one another to detect uniquely expressed genes. Based on default parameters, only genes that were enriched and expressed in a minimum of 10% of each population (min.pct = 0.1) and with a log fold difference larger than 0.25 (logfc.threshold = 0.25) were considered. We used a Wilcoxon rank sum test to perform the analysis and confirmed with another algorithm called Model-based Analysis of Single-cell Transcriptomics (MAST) using the {FindAllMarkers} function on default settings. A differentially expressed gene (DEG) is defined as any gene expressed in at least 10% of the cells, which has a p-value <0.001 and a >1.5x average fold change from all other clusters being tested. Additionally, cell clusters were defined to have at least 10 DEGs that were unique when compared to other clusters. These DEGs per cluster were plotted using {DimPlot} and {FeaturePlot} functions in Seurat for visualization in UMAP plot. Using the {VlnPlot} function, we generated Violin plots to look at gene expression across clusters, and {DoHeatmap} to generate heatmaps of the top 20 DEGs. Finally, we annotated each cell type by extensive literature reading and searching for the specific gene expression patterns.

Single-cell trajectory analysis

We used Monocle3 (v.0.2.3.0) R package (https://cole-trapnell-lab.github.io/monocle3/) [52] to investigate inferred developmental trajectories between interdental cell subsets and order cells in pseudotime based on their transcriptional similarities, in an unbiased manner. The subset data, previously scaled, normalized and clustered by the Seurat tool, were imported into Monocle3 using {new_cell_data_set} function. Monocle3 was run on our normalized counts matrix for the subclustered interdental cell data (IdC_Control and IdC_Dox). The data were subject to UMAP dimensional reduction and cell clustering using the {cluster_cells} function. A principal graph was plotted through the UMAP coordinates using the {learn_graph} function that represents the path from IdC_Control to IdC_Dox. This principal graph was further used to order cells in pseudotime using the {ordercells} function in Monocle3. Following that, we defined the population of IdC_Control cells as the root cell state (the starting point) to further investigate genes allowing IdC_Dox cells the ability to divide and regenerate. DEGs between IdC_Control and IdC_Dox clusters used to generate hypothetical developmental relationships were determined using {graph_test} function. Monocle3 identified modules of co-regulated genes within our selected clusters using the function graph test to identify variable genes in the data based on Moran's I statistic. We retained the genes that had a significant q-value (< 0.001) from the auto-correlation analysis, grouped these genes into modules using UMAP and Louvain community analysis, and then genes with the greatest q-values were plotted on a heatmap using a proposed function {pheatmap}.

Pathway analysis

DAVID v6.8 (https://david.ncifcrf.gov/) [30,31] was applied using default settings to identify enriched pathways based on the DEGs between two groups or clusters. We used pathway gene sets from the biological processes of Gene Ontology (http://www.geneontology.org/) or the Hallmark pathway collection from Molecular Signatures Database (MSigDB; http://www.gsea-msigdb.org/gsea/).

Data availability

Raw and pre-processed single-cell sequence data that support the findings of this study are available through the National Center for Biotechnology Information Gene Expression Omnibus (NCBI GEO) (GSE???). R scripts for data processing are available through https://github.com/ZYChenLab/HC_Regeneration**.** There is no restriction on the use of the code or data for non-profit academic organizations.

Partial reprogramming *in vitro* for HC regeneration.

In the rtTA/tet-*Myc*/tet-*NICD* mouse model, cochleae were treated with Dox (Sigma, 2 μg/ml final concentration); In the Sox2/tdT/rtTA/tet-*Myc*/tet-*NICD* mouse model, cochleae were treated with Dox (Sigma, 2 μg/ml final concentration) and 4-Hydroxytamoxifen (Tm, Sigma) (20ng/ml); in the rtTA/tet-*Myc* and rtTA/tet-*Myc*/Atoh1-GFP mouse models, cochleae were treated with Dox (Sigma, 2 μg/ml final concentration) and VPA (1.5 mM); in the Sox2/tdT/rtTA/tet-*Myc* mouse model, cochleae were treated with 4-Hydroxytamoxifen (20ng/ml), Dox (Sigma, 2 μg/ml) and VPA (Sigma, 1.5 mM); in the rtTA/tet-*NICD* mouse model, cochleae were treated with Dox (Sigma, 2 μg/ml final concentration), LiCl (Sigma, 8mM), FSK (Tocris Bioscience, 20μM), siFIR (Santa Cruz Bio-technology, 0.02 μM), and siMxi1 (Santa Cruz Bio-technology, 0.02 μM); in the Sox2/tdT/rtTA/tet-*NICD* mouse model, cochleae were treated with 4-Hydroxytamoxifen (20ng/ml), Dox (Sigma, 2 μg/ml final concentration), LiCl (8mM), Forskolin (FSK) (20μM), siFIR (Puf 60, Gene ID: 67959) (0.02 μM), and siMxi1 (Gene ID: 17859) (0.02 μM); in the Atoh1-GFP mouse model, cochleae were treated with VPA (1.5 mM), LiCl (8mM), FSK (20μM), siFIR (0.02 μM), and siMxi1 (0.02 μM) for 4 days, followed by Ad.*Atoh1* (6×10^{10} pfu/ml) infection overnight. siRNAs were delivered following the manufacturer's instructions (Polyplus-transfection; 89129-920). The controls were cultured adult cochleae of the same genotype treated with vehicle (sterile water with 0.1% DMSO) plus Ad.Atoh1. The culture was placed into fresh medium for an additional 10-14 days. Cochleae were harvested and decalcified before immunohistochemistry.

Lineage tracing

Cochlear tissues from 4- to 6-week-old Sox2-CreER/tdT mice, Sox2-CreER/tdT/rtTA/tet-*MYC* quad mice, Sox2-CreER/tdT/rtTA/tet-*NICD* quad mice, and Sox2-CreER/tdT/rtTA/tet-*MYC*/tet-*NICD* quint mice were dissected for culture. 4-Hydroxytamoxifen (20 ng/mL) was added to cultures on day 0 to activate Cre for lineage tracing studies. Ad.*Atoh1* virus was added to the medium for 16 to 24 hours at a concentration of $6x10^{10}$ pfu/ml.

Trans-tympanic Injection of chemicals *in vivo.*

All adult mice used were between 4 and 6 weeks old. Trans-tympanic injections were performed 7 days after the subcutaneous injection of Kanamycin (1mg/g; Sigma) followed by intraperitoneal injection of Furosemide (0.3mg/g; Hospira Inc) 30 min later. Mice were anesthetized by intraperitoneal injection of xylazine (10 mg/kg) and ketamine (100 mg/kg). Trans-tympanic injections were conducted with 5μl chemical combinations of VPA (5mg/ml), LiCl (40mM), FSK (50μg/ml), siFIR (0.6μg/10μl), and siMxi1 (0.6μg/10μl), or vehicle (sterile water with 0.5% DMSO). Chemicals or vehicle were injected into one ear through the tympanic membrane (TM) in

mice. Microforceps were used to retract the skin and visualize the medial superior fold adjacent to the TM. A Hamilton syringe with 33G needle was used to inject drugs trans-tympanically.

Viral Injection *in vivo*.

All surgical procedures were done in a clean, dedicated space. Instruments were thoroughly cleaned with 70% ethanol and autoclaved before surgery. Mice were anesthetized by intraperitoneal injection of xylazine (10 mg/kg) and ketamine (100 mg/kg). For viral injection, cochleostomy was performed on the anesthetized mice by opening the bulla, and adenovirus with a titer of 5×10^{12} pfu/ml was injected into the middle turn of the scala media by a pressure-controlled motorized microinjector at a speed of 3 nl/sec. A total of 1 µl of adenovirus was injected into each cochlea.

Scanning Electron Microscopy.

Following dissection, the tissue was harvested and immersed in 2.5% glutaraldehyde in 0.1 M cacodylate buffer (EMS) supplemented with 2 mM $CaCl_2$ at room temperature for 1.5-2 hours on a tissue rotator. Samples were then washed with distilled water 3 times and additional dissection was performed post-fixation, as needed. The samples were then rinsed with 0.1 M sodium cacodylate buffer 3 times for 10 min and treated with 1% osmium tetroxide (O) for 1 h, followed by a thorough rinse with distilled water 3 times for 10 min each, and treated with saturated thiocarbohydrazide (T) in distilled water for 30 min. This treatment was repeated, followed by an additional 1% osmium tetroxide step, yielding a treatment order of O-T-O-T-O. Following the final treatment and another round of washes, samples were transferred to 20 ml scintillation vials in 2 ml distilled water for dehydration with ethanol by adding 50 µl of 100% ethanol to the vial, then doubling the added volume every 10 min. Once the vial was full, samples were transferred to a 100% ethanol, then critical point dried from liquid CO_2 (Tousimis Autosamdri 815). The samples were then mounted on aluminum specimen stubs with a carbon tape, spatter-coated with 4.5 nm of platinum (Leica EM ACE600) and observed with a field emission SEM (Hitachi S-4700).

Statistical analysis

The Prism 8 statistical package (GraphPad Software, Inc) was used in data processing. To count HCs upon partial-reprogramming followed by activation of Atoh1 in vitro, multiple regions from the apex (80-100% of the length of cochlear duct from the hook) were included. Briefly, new HC-like cells generated from Hensen cell region, Deiters' cell region, pillar cell region, inner phalangeal and inner sulcus cell region were all included in the "SE" region; the cells generated from limbus region were included in the "Lib" region.

To count the number of HCs upon VLFsiFsiM in vivo, the apex (80-100% of the length of cochlear duct from the hook); the apex-mid (60-80% of the length of cochlear duct from the hook) and mid (50-60% of the length of cochlear duct from the hook) were included. The injection sites were close to the mid turn. ESPN+ HCs were counted and the HC density was calculated as the average number of HCs per 100 µm for each cochlea. Controls were sterile water plus 0.5% DMSO-injected cochleae. Multiple cochleae were used for each counting and in statistical analysis.

Data were presented as mean ± SEM. Two-tailed Student's t-test was used to compare two groups ($p<0.05$ was considered significant). ANOVA analysis with Turkey's multiple comparisons test was used to compare three or more groups ($p<0.05$ was considered significant).

Data availability

The source data underlying Fig 1, 4, 5, Supplementary Fig 1, 2, 7, 10, 11 are provided as a Source Data file.

Figure Legends

Figure 1.

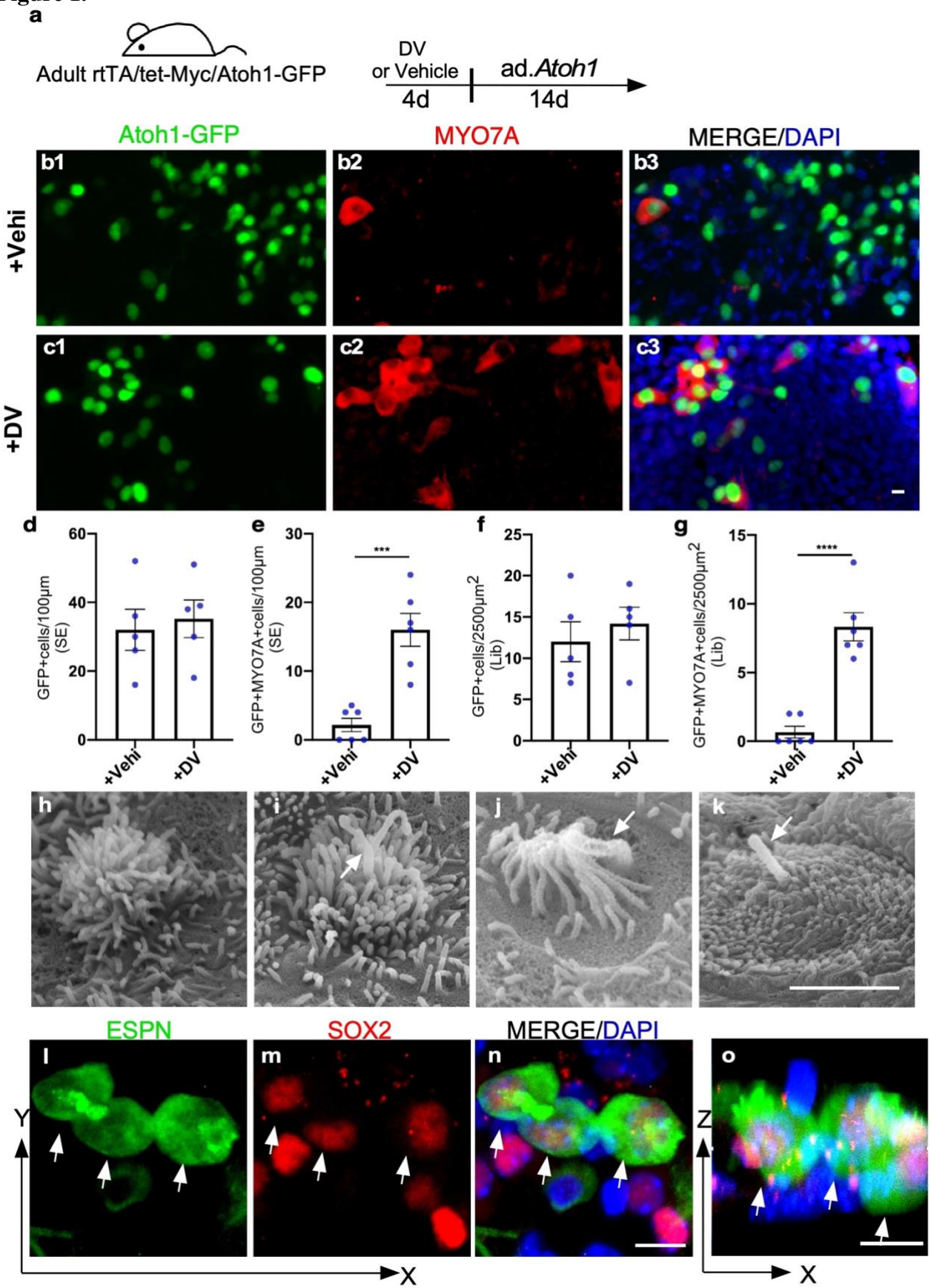

Figure 1. VPA effectively replaces *NICD* to reprogram adult SCs for HC regeneration. a. A schematic diagram illustrating the experimental procedure of the cultured adult cochleae treated transiently by Dox to induce *Myc* and VPA to activate *NICD* (DV) and HC induction by Ad.*Atoh1*. **b, c.** Vehicle (sterile water)/Ad.*Atoh1* or Dox/VPA/Ad.*Atoh1* treated adult (P30) rtTA/tet-*Myc*/Atoh1-GFP mice cochlear samples were labelled with MYO7A/GFP. Numerous HCs ($MYO7A^+$/$Atoh1\text{-}GFP^+$) were seen in the DV treated group and occasional HCs were seen in the control sample. **d-g.** Quantification and comparison of GFP+ cells and regenerated HC-like cells in the apical turn of the cultured cochleae between Dox/VPA/Ad.*Atoh1* treated and Vehicle/Ad.*Atoh1* treated groups. Similar number of GFP^+ cells, i.e. the Ad.*Atoh1* infected cells, were seen in the DV and control cochleae (d, f). Significantly more HCs were seen in the DV treated than in control samples (e, g). ***p<0.001, ****p<0.0001, two-tailed unpaired Student's t-test. Error bar, mean ± SEM, n=5. **h-k.** Images of scanning electron microscopy (SEM) showing immature stereocilia from new HCs in rtTA/tet-*Myc*/Atoh1-GFP cochlea treated with Dox/VPA and Ad.*Atoh1 in vitro*. Arrows point to kinocilia. **l-o**. Dox/VPA/Ad.*Atoh1* treated adult (P30) rtTA/tet-*Myc* mouse cochlear samples were stained ESPN/SOX2. Arrows point to the $SOX2^+$/$ESPN^+$ double positive HCs. Scale bar in h-k: 2 μm; l-o: 10 μm.

Figure 2.

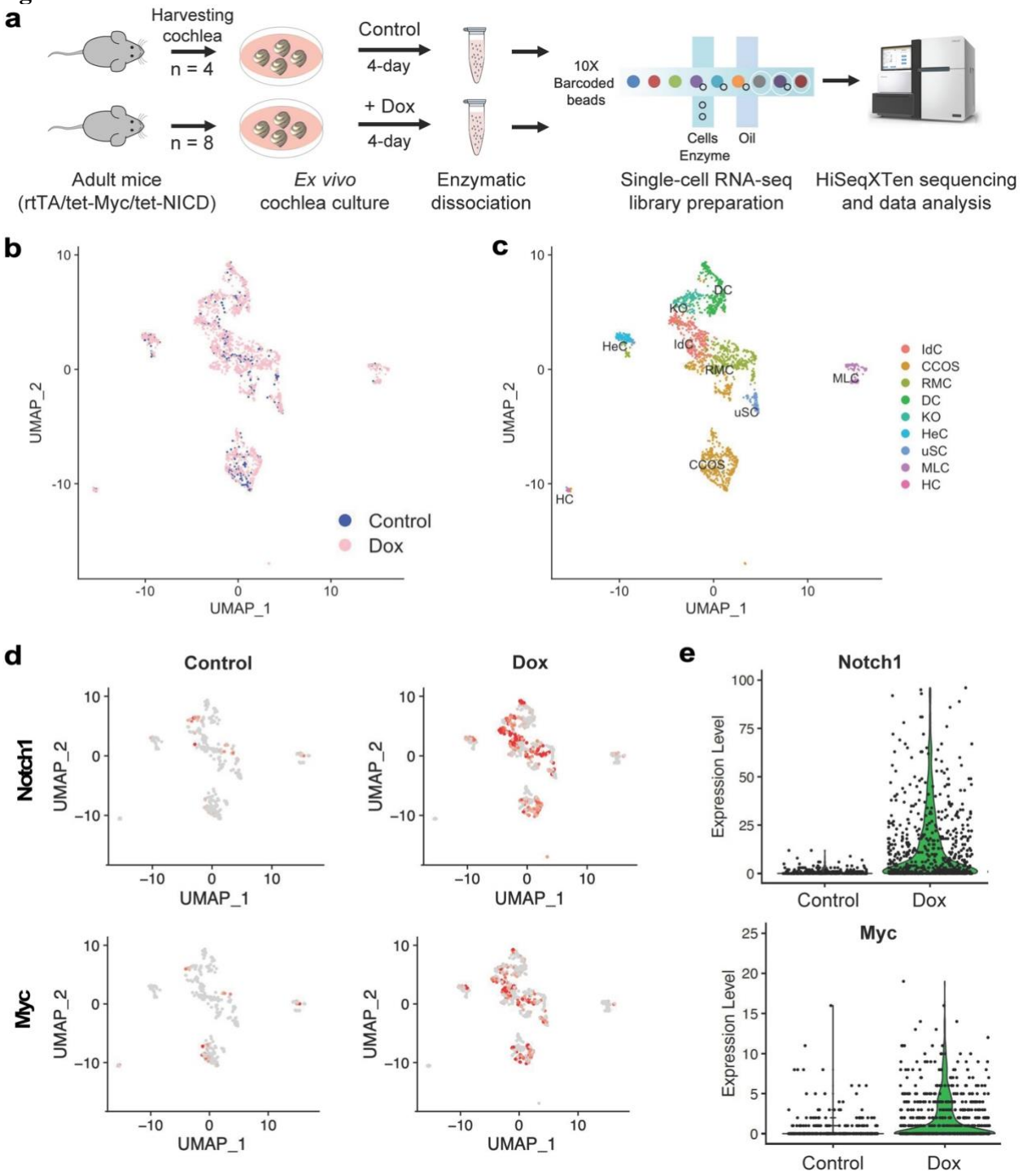

Figure 2. Single-cell RNA sequencing identified putative cell types across the sensory epithelium from mouse cochlear explant culture. a. Schematic diagram depicting the experimental setup for collection and processing of cochlear explants for the 10X Genomics Chromium Single Cell 3' Gene Expression workflow. **b.** UMAP plot showing the putative clusters from the integrated analysis of Control and Dox groups. **c.** UMAP plot of 2395 cells displaying each cell colored according to putative cluster assignment. **d.** UMAPs colored by the normalized log-transformed expression of Notch1 and Myc, proving Dox-induced transgene expression. Color key from gray to red indicates relative expression levels from low to high. **e.** Violin plots illustrating differential expression of Notch1 and Myc transgenes across the cells from Control and Dox-induced samples.

Figure 3

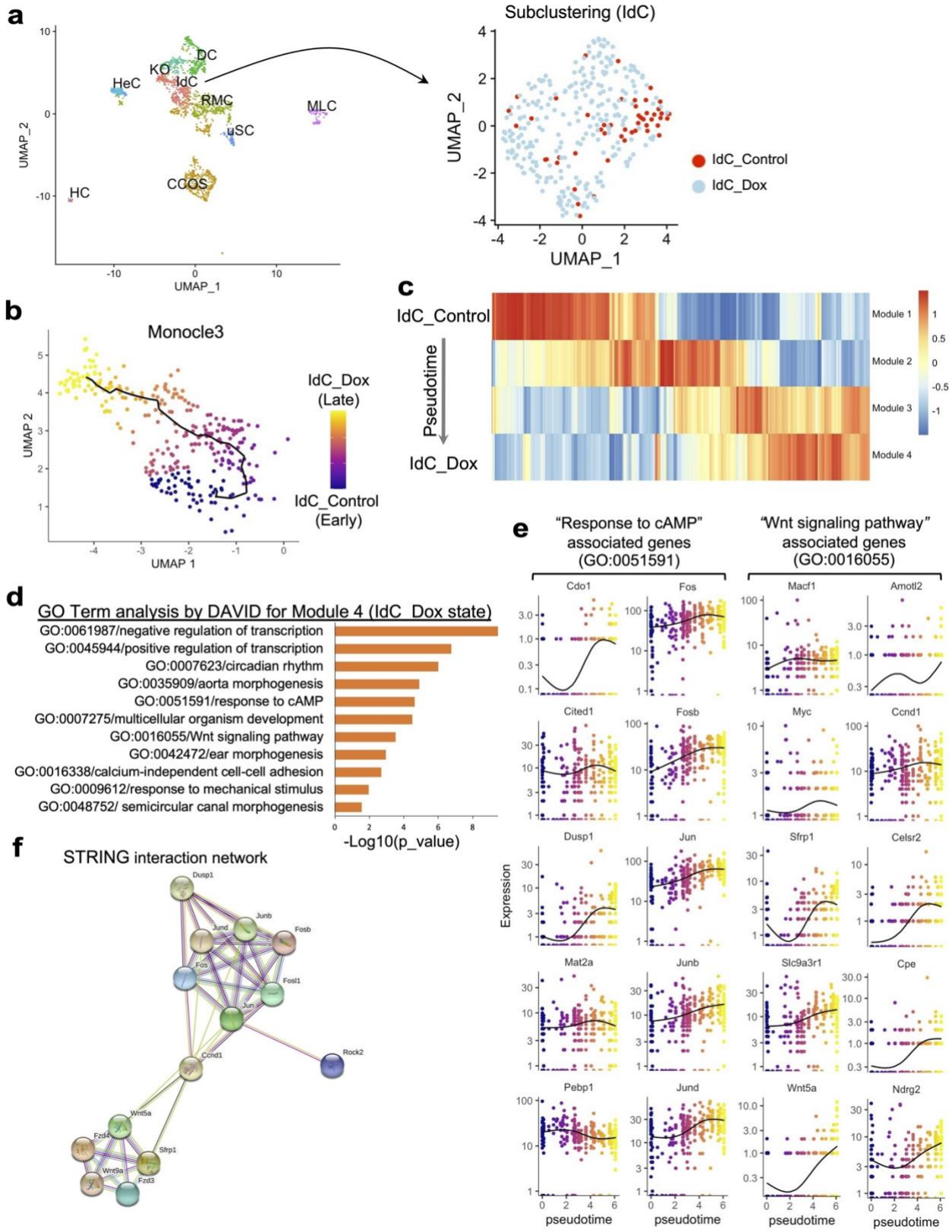

Figure 3. Computational lineage modeling analysis for the reprogramming trajectory for the interdental cell (IdC) cluster. a. Subclustering of the interdental cells (IdC) showing distinct accumulation of Control (red), and surrounded by Dox-induced sample-derived IdC cells (light blue). **b.** Construction of a pseudotime trajectory of the IdC subcluster from Control to Dox-administered samples, with the black line showing the path of pseudotime, and UMAP plots are

colored according to pseudotime. **c.** Expression changes of the co-regulated genes within each module generated by Monocle3 analysis. The modules are consisted of genes clustered according to the correlation of expression levels. **d.** Gene Ontology analysis of Module 4 by DAVID using the genes whose expression changed significantly over pseudotime. The GO terms with p value less than 0.05 were considered significantly enriched by the query genes. **e.** Kinetic plots showing the relative expression of the top 10 of Response to cAMP and Wnt Signaling Pathway-associated genes over the pseudotime. **f.** A functional interaction network of the key genes from the Response to cAMP and Wnt Signaling Pathways. The nodes represent proteins, and the colored lines represent interactions between proteins. Presence of the more lines denotes the greater the degree of connection.

Figure 4.

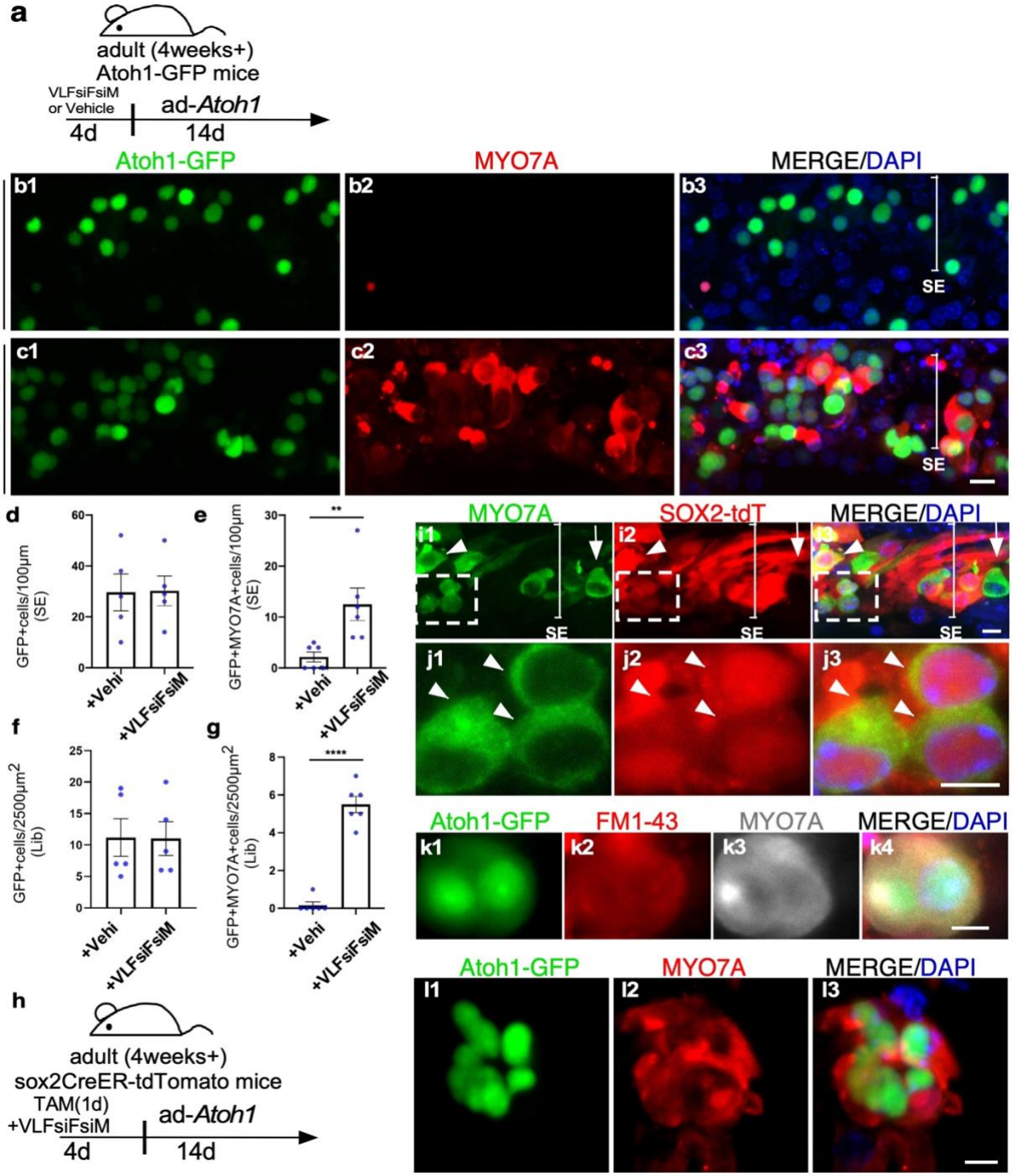

Figure 4. A cocktail of siRNAs and small molecules to replace MYC/NICD in reprogramming for HC regeneration in adult cochlea *in vitro*. a. A schematic diagram illustrating the experimental procedure of VLFsiFsiM/Ad.*Atoh1* induced HC regeneration. **b, c.** The cocktail (VLFsiFsiM)/Ad.*Atoh1* or Vehicle/Ad.*Atoh1* treated adult (P30) *Atoh1*-GFP mice cochlear samples were labeled with MYO7A (red)/ Atoh1-GFP (green) in the sensory epithelial region. Numerous HCs (MYO7A$^+$) were seen in the VLFsiFsiM/Ad.*Atoh1* treated cochlea. **d-g.** Quantification and comparison of regenerated HCs in the apical turn of the cultured cochleae between VLFsiFsiM/Ad.*Atoh1* treated and Vehicle/Ad.*Atoh1* treated groups. Significantly more HCs were regenerated in the VLFsiFsiM/Ad.*Atoh1* treated than Vehicle/Ad.*Atoh1* treated samples (e, g), whereas the number of Ad.*Atoh1* infected cells (GFP$^+$) was similar. **h.** A schematic diagram illustrating the experimental procedure of lineage tracing for new HCs after VLFsiFsiM/Ad.*Atoh1*

treatment. **i.** In the cultured Sox2CreER/tdT adult cochlea, Tamoxifen (Tamo) induced tdT in the SCs which transdifferentiated to HCs by VLFsiFsiM/Ad.*Atoh1* treatment, shown by MYO7A$^+$/Sox2-tdT$^+$ labeling. The arrow indicates an existing HC, which was MYO7A$^+$/Sox2-tdT$^-$. The arrowhead indicates a regenerated HC, shown by MYO7A$^+$/Sox2-tdT$^+$ labeling. **j.** Enlarge inset from H to show MYO7A$^+$/Sox2-tdT$^+$ cells (arrows). **k.** VLFsiFsiM/Ad.*Atoh1* treated adult (P30) *Atoh1*-GFP mouse cochlear samples showed infected cells (GFP$^+$) that transdifferentiated to HC (MYO7A$^+$) and were able to take up FM1-43. **l.** A cluster of HCs (MYO7A$^+$) was seen in the VLFsiFsiM/Ad.*Atoh1* treated adult cochlea. T, Tamo: 4-hydroxytamoxifen. V: VPA; L:LiCl; F:FSK; siF: siFIR; siM: siMxi1. **$p < 0.01$, ****$p < 0.0001$, Student's t-test. Error bar, mean ± SEM; N=5-6 in each group. Source data are provided as a Source Data file. Scale bars: 10 μm.

Figure 5.

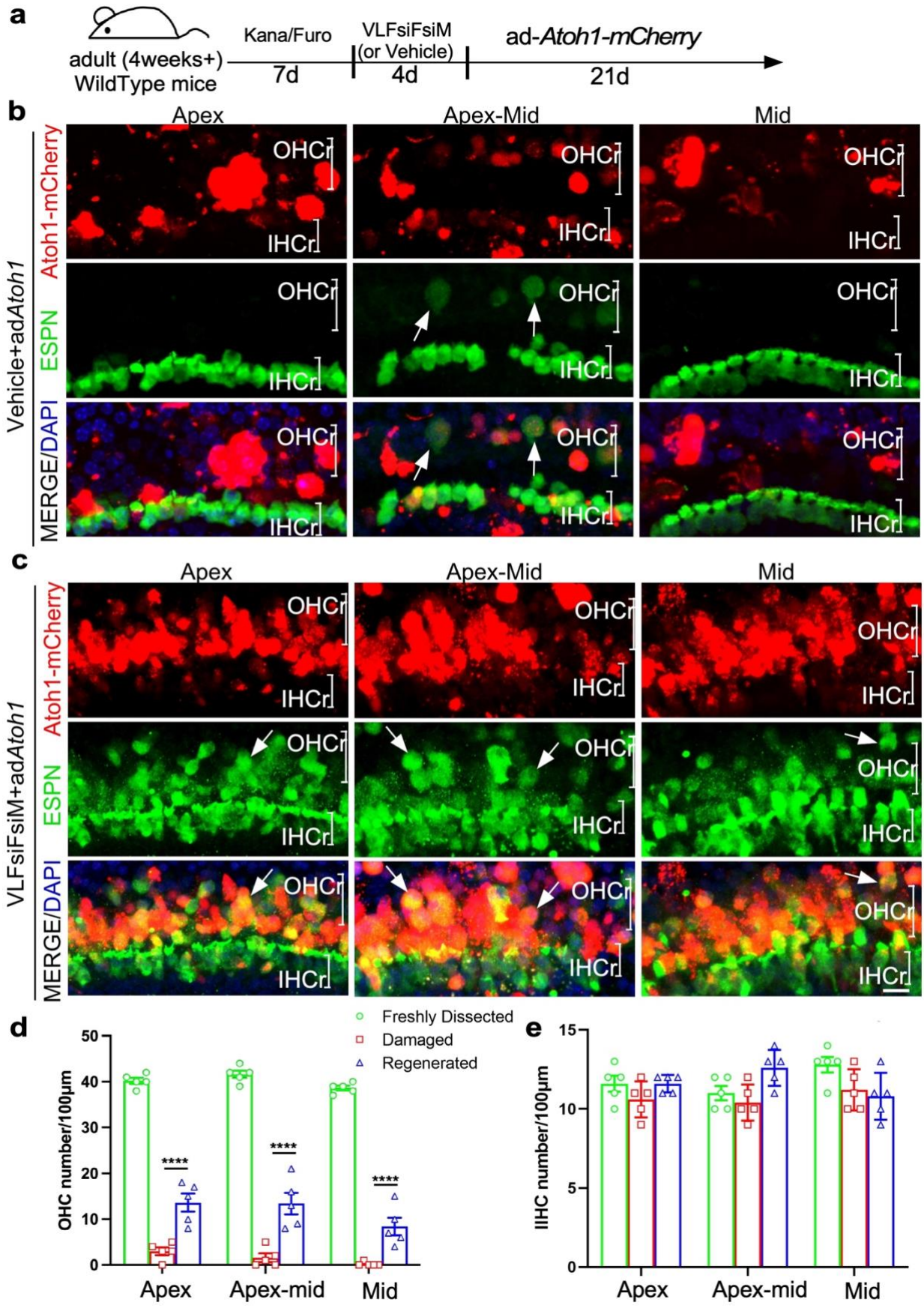
a
adult (4weeks+)
WildType mice
Kana/Furo
7d
VLFsiFsiM
(or Vehicle)
4d
ad-Atoh1-mCherry
21d
b
Apex
Apex-Mid
Mid
Vehicle+adAtoh1
Atoh1-mCherry
ESPN
MERGE/DAPI
OHCr
IHCr
c
Apex
Apex-Mid
Mid
VLFsiFsiM+adAtoh1
Atoh1-mCherry
ESPN
MERGE/DAPI
OHCr
IHCr
d
Freshly Dissected
Damaged
Regenerated
OHC number/100μm
50
40
30
20
10
0
****
****
****
Apex
Apex-mid
Mid
e
IIHC number/100μm
15
10
5
0
Apex
Apex-mid
Mid

Figure 5. Regeneration of hair cells in a mouse model with HC loss *in vivo*. a. A schematic diagram illustrating the experimental procedure that adult C57BL/6j mice were treated by Kanamycin/Furosemide (Kana/Furo) to kill hair cells, with the subsequent delivery of the cocktail (VLFsiFsiM) or Vehicle (sterile water plus 0.1%DMSO) into the middle ear space, followed by the injection of Ad.*Atoh1-mCherry* into the inner ear by cochleostomy. **b.** After Kana/Furo treatment, Vehicles/Ad.*Atoh1-mCherry* treated adult C57BL/6j cochleae showed scarce hair cells (arrows, $ESPN^+/mCherry^+$) in the outer hair cell region (OHCr) of the apex-middle turn. **c.** After Kana/Furo treatment, cocktail/Ad.*Atoh1-mCherry* treated adult C57BL/6j cochleae showed many hair cells (arrows, $ESPN^+/mCherry^+$) in the outer hair cell regions (OHCr) from the apex to the mid-turn. **d.** Quantification and comparison of regenerated HCs showed a significant increase in the HC number in the OHCr in the cocktail treated samples compared to the Vehicle treated samples. **e.** Quantification and comparison showed a comparable HC number in the IHC region in the cocktail treated, Vehicle treated and WT control cochlear samples. D: Dox; L: LiCl; F: FSK; siF: siFIR; siM: siMxi1. $^{**}p < 0.01$, $^{***}p < 0.001$, $^{****}p < 0.0001$, two-tailed unpaired Student's t-test. Error bar, mean ± SEM; N=5-6 in each group. Source data are provided as a Source Data file. Scale bars: 10 μm.

Figure 6.

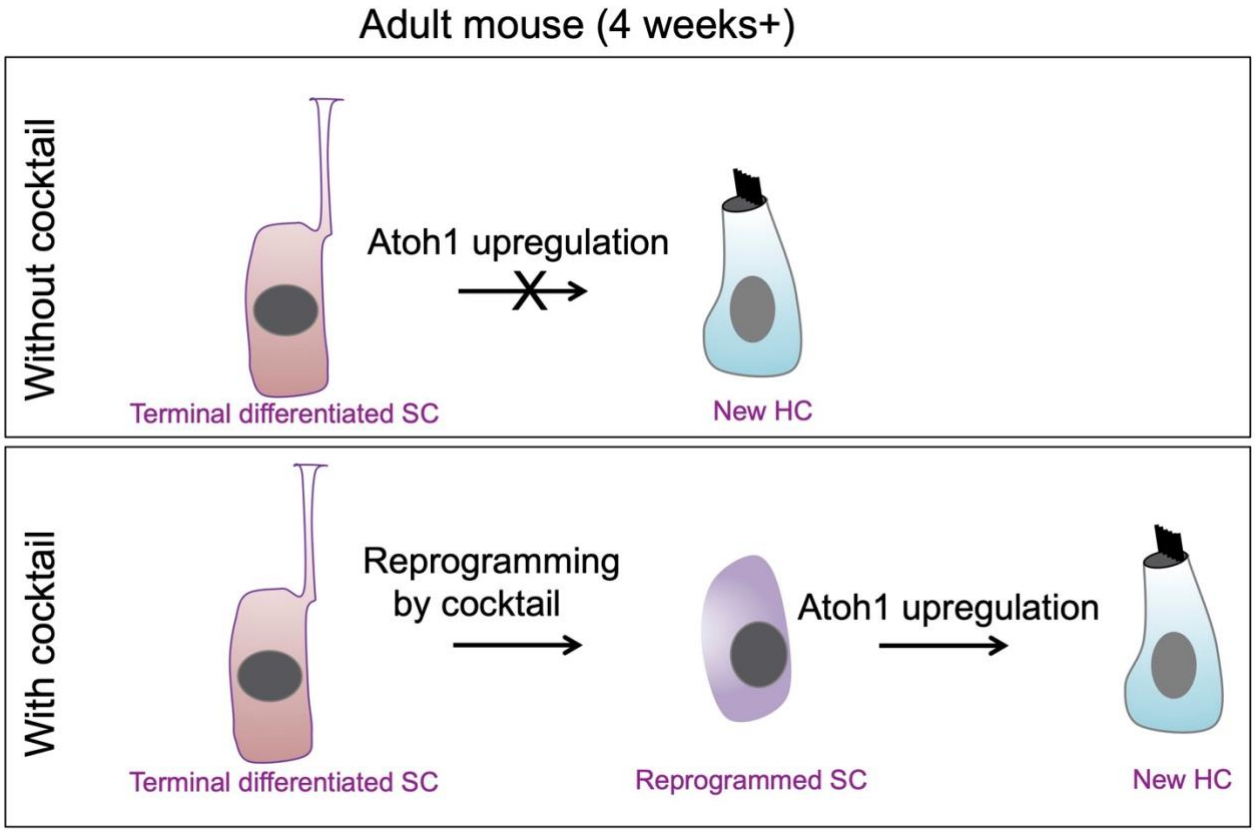

Figure 6. A schematic diagram summarizing the working model for SC reprogramming by the drug-like molecules and the HC regeneration.

REFERENCES

1 Corwin, J. T. & Cotanche, D. A. Regeneration of sensory hair cells after acoustic trauma. *Science* **240**, 1772-1774 (1988).

2 Ryals, B. M. & Rubel, E. W. Hair cell regeneration after acoustic trauma in adult Coturnix quail. *Science* **240**, 1774-1776 (1988).

3 Hudspeth, A. J. How hearing happens. *Neuron* **19**, 947-950, doi:10.1016/s0896-6273(00)80385-2 (1997).

4 Warchol, M. E., Lambert, P. R., Goldstein, B. J., Forge, A. & Corwin, J. T. Regenerative proliferation in inner ear sensory epithelia from adult guinea pigs and humans. *Science* **259**, 1619-1622 (1993).

5 Forge, A., Li, L., Corwin, J. T. & Nevill, G. Ultrastructural evidence for hair cell regeneration in the mammalian inner ear. *Science* **259**, 1616-1619 (1993).

6 Corwin, J. T. Postembryonic production and aging in inner ear hair cells in sharks. *The Journal of comparative neurology* **201**, 541-553, doi:10.1002/cne.902010406 (1981).

7 Jones, J. E. & Corwin, J. T. Replacement of lateral line sensory organs during tail regeneration in salamanders: identification of progenitor cells and analysis of leukocyte activity. *J Neurosci* **13**, 1022-1034 (1993).

8 Zheng, J. L. & Gao, W. Q. Overexpression of Math1 induces robust production of extra hair cells in postnatal rat inner ears. *Nat Neurosci* **3**, 580-586, doi:10.1038/75753 (2000).

9 Liu, Z. *et al.* Age-dependent in vivo conversion of mouse cochlear pillar and Deiters' cells to immature hair cells by Atoh1 ectopic expression. *J Neurosci* **32**, 6600-6610, doi:10.1523/JNEUROSCI.0818-12.2012 (2012).

10 Li, X. J., Morgan, C., Goff, L. A. & Doetzlhofer, A. Follistatin promotes LIN28B-mediated supporting cell reprogramming and hair cell regeneration in the murine cochlea. *Sci Adv* **8**, eabj7651, doi:10.1126/sciadv.abj7651 (2022).

11 Chen, Y. *et al.* Hedgehog Signaling Promotes the Proliferation and Subsequent Hair Cell Formation of Progenitor Cells in the Neonatal Mouse Cochlea. *Front Mol Neurosci* **10**, 426, doi:10.3389/fnmol.2017.00426 (2017).

12 Lu, N. *et al.* Sonic hedgehog initiates cochlear hair cell regeneration through downregulation of retinoblastoma protein. *Biochem Biophys Res Commun* **430**, 700-705, doi:10.1016/j.bbrc.2012.11.088 (2013).

13 Zhang, J. *et al.* ERBB2 signaling drives supporting cell proliferation in vitro and apparent supernumerary hair cell formation in vivo in the neonatal mouse cochlea. *Eur J Neurosci* **48**, 3299-3316, doi:10.1111/ejn.14183 (2018).

14 Shu, Y. *et al.* Renewed proliferation in adult mouse cochlea and regeneration of hair cells. *Nature communications* **10**, 5530, doi:10.1038/s41467-019-13157-7 (2019).

15 Sage, C. *et al.* Essential role of retinoblastoma protein in mammalian hair cell development and hearing. *Proc Natl Acad Sci U S A* **103**, 7345-7350, doi:10.1073/pnas.0510631103 (2006).

16 Greenblatt, D. Y. *et al.* Valproic acid activates notch-1 signaling and regulates the neuroendocrine phenotype in carcinoid cancer cells. *Oncologist* **12**, 942-951, doi:10.1634/theoncologist.12-8-942 (2007).

17 Yin, X. *et al.* Niche-independent high-purity cultures of Lgr5+ intestinal stem cells and their progeny. *Nat Methods* **11**, 106-112, doi:10.1038/nmeth.2737 (2014).

18 McLean, W. J. *et al.* Clonal Expansion of Lgr5-Positive Cells from Mammalian Cochlea and High-Purity Generation of Sensory Hair Cells. *Cell Rep* **18**, 1917-1929, doi:10.1016/j.celrep.2017.01.066 (2017).

19 Zine, A. & Romand, R. Development of the auditory receptors of the rat: a SEM study. *Brain Res* **721**, 49-58, doi:10.1016/0006-8993(96)00147-3 (1996).
20 Schreiber-Agus, N. *et al.* An amino-terminal domain of Mxi1 mediates anti-Myc oncogenic activity and interacts with a homolog of the yeast transcriptional repressor SIN3. *Cell* **80**, 777-786, doi:10.1016/0092-8674(95)90356-9 (1995).
21 Matsushita, K. *et al.* An essential role of alternative splicing of c-myc suppressor FUSE-binding protein-interacting repressor in carcinogenesis. *Cancer Res* **66**, 1409-1417, doi:10.1158/0008-5472.CAN-04-4459 (2006).
22 Stuart, T. *et al.* Comprehensive Integration of Single-Cell Data. *Cell* **177**, 1888-1902 e1821, doi:10.1016/j.cell.2019.05.031 (2019).
23 Burns, J. C., Kelly, M. C., Hoa, M., Morell, R. J. & Kelley, M. W. Single-cell RNA-Seq resolves cellular complexity in sensory organs from the neonatal inner ear. *Nature communications* **6**, 8557, doi:10.1038/ncomms9557 (2015).
24 Hoa, M. *et al.* Characterizing Adult Cochlear Supporting Cell Transcriptional Diversity Using Single-Cell RNA-Seq: Validation in the Adult Mouse and Translational Implications for the Adult Human Cochlea. *Front Mol Neurosci* **13**, 13, doi:10.3389/fnmol.2020.00013 (2020).
25 Kolla, L. *et al.* Characterization of the development of the mouse cochlear epithelium at the single cell level. *Nature communications* **11**, 2389, doi:10.1038/s41467-020-16113-y (2020).
26 Ranum, P. T. *et al.* Insights into the Biology of Hearing and Deafness Revealed by Single-Cell RNA Sequencing. *Cell Rep* **26**, 3160-3171 e3163, doi:10.1016/j.celrep.2019.02.053 (2019).
27 Yu, K. S. *et al.* Development of the Mouse and Human Cochlea at Single Cell Resolution. *bioRxiv*, 739680, doi:10.1101/739680 (2019).
28 Liberzon, A. *et al.* Molecular signatures database (MSigDB) 3.0. *Bioinformatics* **27**, 1739-1740, doi:10.1093/bioinformatics/btr260 (2011).
29 Subramanian, A. *et al.* Gene set enrichment analysis: a knowledge-based approach for interpreting genome-wide expression profiles. *Proc Natl Acad Sci U S A* **102**, 15545-15550, doi:10.1073/pnas.0506580102 (2005).
30 Huang da, W., Sherman, B. T. & Lempicki, R. A. Systematic and integrative analysis of large gene lists using DAVID bioinformatics resources. *Nature protocols* **4**, 44-57, doi:10.1038/nprot.2008.211 (2009).
31 Huang da, W., Sherman, B. T. & Lempicki, R. A. Bioinformatics enrichment tools: paths toward the comprehensive functional analysis of large gene lists. *Nucleic acids research* **37**, 1-13, doi:10.1093/nar/gkn923 (2009).
32 Szklarczyk, D. *et al.* STRING v11: protein-protein association networks with increased coverage, supporting functional discovery in genome-wide experimental datasets. *Nucleic acids research* **47**, D607-D613, doi:10.1093/nar/gky1131 (2019).
33 Muncie, J. M. *et al.* Mechanical Tension Promotes Formation of Gastrulation-like Nodes and Patterns Mesoderm Specification in Human Embryonic Stem Cells. *Dev Cell* **55**, 679-694 e611, doi:10.1016/j.devcel.2020.10.015 (2020).
34 Kleinboelting, S. *et al.* Bithionol Potently Inhibits Human Soluble Adenylyl Cyclase through Binding to the Allosteric Activator Site. *J Biol Chem* **291**, 9776-9784, doi:10.1074/jbc.M115.708255 (2016).
35 Sage, C. *et al.* Proliferation of functional hair cells in vivo in the absence of the retinoblastoma protein. *Science* **307**, 1114-1118, doi:10.1126/science.1106642 (2005).

36 Walters, B. J. *et al.* In Vivo Interplay between p27(Kip1), GATA3, ATOH1, and POU4F3 Converts Non-sensory Cells to Hair Cells in Adult Mice. *Cell Rep* **19**, 307-320, doi:10.1016/j.celrep.2017.03.044 (2017).
37 White, P. M., Doetzlhofer, A., Lee, Y. S., Groves, A. K. & Segil, N. Mammalian cochlear supporting cells can divide and trans-differentiate into hair cells. *Nature* **441**, 984-987, doi:10.1038/nature04849 (2006).
38 Woods, C., Montcouquiol, M. & Kelley, M. W. Math1 regulates development of the sensory epithelium in the mammalian cochlea. *Nat Neurosci* **7**, 1310-1318, doi:10.1038/nn1349 (2004).
39 Baek, S. *et al.* Single-cell transcriptome analysis reveals three sequential phases of gene expression during zebrafish sensory hair cell regeneration. *Dev Cell* **57**, 799-819 e796, doi:10.1016/j.devcel.2022.03.001 (2022).
40 Li, W. *et al.* Notch inhibition induces mitotically generated hair cells in mammalian cochleae via activating the Wnt pathway. *Proc Natl Acad Sci U S A* **112**, 166-171, doi:10.1073/pnas.1415901112 (2015).
41 Jacques, B. E. *et al.* A dual function for canonical Wnt/beta-catenin signaling in the developing mammalian cochlea. *Development* **139**, 4395-4404, doi:10.1242/dev.080358 (2012).
42 Wang, Q. *et al.* Lithium, an anti-psychotic drug, greatly enhances the generation of induced pluripotent stem cells. *Cell Res* **21**, 1424-1435, doi:10.1038/cr.2011.108 (2011).
43 Li, K. *et al.* Small molecules facilitate the reprogramming of mouse fibroblasts into pancreatic lineages. *Cell Stem Cell* **14**, 228-236, doi:10.1016/j.stem.2014.01.006 (2014).
44 Muncan, V. *et al.* Rapid loss of intestinal crypts upon conditional deletion of the Wnt/Tcf-4 target gene c-Myc. *Mol Cell Biol* **26**, 8418-8426, doi:10.1128/MCB.00821-06 (2006).
45 Shu, W. *et al.* Wnt/beta-catenin signaling acts upstream of N-myc, BMP4, and FGF signaling to regulate proximal-distal patterning in the lung. *Dev Biol* **283**, 226-239, doi:10.1016/j.ydbio.2005.04.014 (2005).
46 Bell, T. J. & Oberholtzer, J. C. cAMP-induced auditory supporting cell proliferation is mediated by ERK MAPK signaling pathway. *J Assoc Res Otolaryngol* **11**, 173-185, doi:10.1007/s10162-009-0205-8 (2010).
47 Navaratnam, D. S., Su, H. S., Scott, S. P. & Oberholtzer, J. C. Proliferation in the auditory receptor epithelium mediated by a cyclic AMP-dependent signaling pathway. *Nat Med* **2**, 1136-1139, doi:10.1038/nm1096-1136 (1996).
48 Montcouquiol, M. & Corwin, J. T. Brief treatments with forskolin enhance s-phase entry in balance epithelia from the ears of rats. *J Neurosci* **21**, 974-982 (2001).
49 Cao, S. *et al.* Chromatin Accessibility Dynamics during Chemical Induction of Pluripotency. *Cell Stem Cell* **22**, 529-542 e525, doi:10.1016/j.stem.2018.03.005 (2018).
50 Hou, P. *et al.* Pluripotent stem cells induced from mouse somatic cells by small-molecule compounds. *Science* **341**, 651-654, doi:10.1126/science.1239278 (2013).
51 Post, Y. *et al.* Snake Venom Gland Organoids. *Cell* **180**, 233-247 e221, doi:10.1016/j.cell.2019.11.038 (2020).
52 Cao, J. *et al.* The single-cell transcriptional landscape of mammalian organogenesis. *Nature* **566**, 496-502, doi:10.1038/s41586-019-0969-x (2019).

Acknowledgements

The authors acknowledge funding from NIH R01DC006908, R56DC006908, UG3TR002636 (Z-Y.C.), DOD W81XWH1810331 (Z-Y.C.), Fredrick and Ines Yeatts hair cell regeneration

fellowship (Z-Y.C.), NIH R01DC017166 (A.A.I.), and Mike Toth Head and Neck Cancer center funds (S. V. S).
We thank Rozenn Riou in helping with operating Chromium Controller (S.V.S. Lab). We thank Stewart C. Silver for the editing of the manuscript.

Author contributions

Y.Z.Q., W.W., V.E. designed and performed experiments, analyzed data, interpreted results and drafted manuscript. V.E. performed single-cell RNA sequencing experiments and bioinformatics data analyses. A.P.R., M.H., C.T., A.A.I performed experiments and analyzed data. S.V.S. analyzed data. Z.Y.C conceived the project, designed experiments, analyzed data, interpreted results and wrote the manuscript. All authors edited the manuscript.

Competing interests: Dr. Zheng-Yi Chen has a financial interest in Salubritas Therapeutics, LLC, which is developing treatments for hearing loss including genome editing, inner ear regeneration, novel delivery and gene therapy.

Additional information

Supplementary information is available for this paper.

Supplementary Files

This is a list of supplementary files associated with this preprint. Click to download.

- Supplementaryinformation.pdf
- TableS1.xlsx
- TableS2.xlsx
- TableS3.xlsx
- TableS4primers.xlsx
- MovieS1.avi
- MovieS2.mov
- ZhengYiChenDataavailabilityReviewerTokens.docx